



Relationship between an M6.6 solar flare and subsequent filament activations

F. Rubio da Costa^{1,3}, F. Zuccarello¹, P. Romano², L. Fletcher³, and N. Labrosse³

¹ Department of Physics and Astronomy, University of Catania. Via S. Sofia 78, 95123, Catania, Italy.

e-mail: frdc@oact.inaf.it

² Catania Astrophysical Observatory, Via S. Sofia 78, 95123, Catania, Italy.

³ Department of Physics and Astronomy, University of Glasgow, Glasgow, G12 8QQ, UK.

Abstract. We study an event which occurred in NOAA 8471, where an M6.6 flare and the activation of two filaments were observed on 28 February 1999. A multi-wavelength study allows us to investigate the behavior of the several features observed at different atmospheric levels, that might be used to answer to the question whether and in what conditions the eruption of filaments can play an active or a passive role in the flare occurrence. Imaging data were acquired by BBSO in the $H\alpha$ line and by TRACE in the 1216, 1600, 171 and 195 Å channels, allowing us to deduce the morphology and temporal evolution of the event and to estimate the $Ly-\alpha$ power. Moreover, in order to study the magnetic topology, the extrapolation of the photospheric magnetic field lines was done assuming potential field and using SOHO/MDI magnetograms.

Key words. Sun: activity – Sun: flares – Sun: filaments – Sun: magnetic fields

1. Introduction

The M6.6 GOES class flare which occurred on 28 February 1999 in active region NOAA 8471, started at 16:31:00 UT and reached its peak at 16:38.35 UT.

A coronal mass ejection (CME) was observed by LASCO/SOHO C2 coronagraph at 17:54:05 UT. The corresponding time of the CME initiation calculated with the height-time measurements is 16:42 UT and it was therefore associated with the M6.6 flare.

We studied the morphological evolution of the M6.6 flare using images and magnetograms provided by the Big Bear Solar Observatory

(BBSO) and images acquired by TRACE at 1600, 1216, 171 and 195 Å during the pre-flare and the maximum phases of the flare. MDI line-of-sight magnetograms were used to deduce the coronal configuration of the magnetic field.

As explained in Rubio da Costa et al. (2009), we can estimate the $Ly-\alpha$ power in this flare by correcting the influence of the 1600 Å TRACE channel from the 1216 Å TRACE channel using the following equation (see Kim et al. (2006) and references therein):

$$I_{Ly\alpha} = A \times I_{1216} + B \times I_{1600} \quad (1)$$

Send offprint requests to: F. Rubio

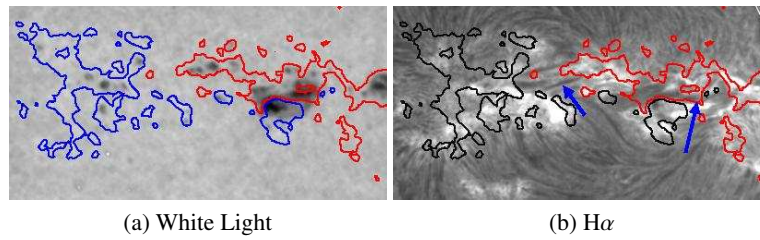


Fig. 1: Positive (red) and negative (blue and black) isocontours of BBSO V Stokes component at ± 200 G, taken at 17:50 over (a): BBSO photospheric image; (b): BBSO $H\alpha$ image.

where A and B parameters are obtained by calibrating TRACE data with spectroscopic data from SUMER ($A = 0.97$ and $B = -0.14$).

We measured the power at the flare footpoints in the TRACE 1216 Å and 1600 Å images taken at 16:36:00 UT and 16:35:53 UT respectively, choosing the flare region using a range between 1200 and 4090 DN, to avoid the saturated pixels. Using the Eq. 1, we estimated that the power in Ly- α at the beginning of the impulsive phase of the flare along the footpoints is 6.8×10^{25} erg s $^{-1}$. This value is greater than the value estimated for an M1.4 class flare (5.6×10^{25} erg s $^{-1}$) studied in a previous work (Rubio da Costa et al. 2009); this is consistent with the fact that the M6.6 class flare is more energetic in X-rays than the M1.4 class flare previously studied.

2. Active region configuration

In Fig. 1a, we overplotted the BBSO line-of-sight magnetogram over the BBSO photospheric image of NOAA 8471 nearest in time: we can see that the main sunspot present in the active region has a δ configuration, with both positive and negative magnetic polarities inside the same penumbra. Overplotting the BBSO line-of-sight magnetogram over the BBSO high resolution $H\alpha$ image nearest in time, we see in Fig. 1b several filaments situated over the photospheric inversion line. In particular, we highlight the presence of a filament in the western part of the active region (filament 1, indicated by the arrow on the right) and of another one in the eastern part (filament 2, indicated by the arrow on the left), because

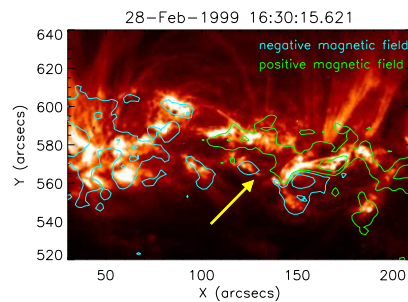


Fig. 2: Positive (green) and negative (blue) isocontours of the magnetic field strength at ± 200 , 1000 G deduced from the MDI magnetogram taken at 16:03 UT over the TRACE 171 Å image acquired at 16:30 UT.

these filaments have a key role in the flaring process and in the CME occurrence.

Overplotting the ± 200 , 1000 G isocontours of MDI magnetogram acquired at 16:03:02 UT over the TRACE 171 Å image acquired at 16:30:15 UT (taking into account the rotation of the Sun, the co-alignment of both images is done by maximizing the cross correlation function with the TRACE 1600 Å as a guide and considering the correction of the SOHO roll angle for this day), we can see in Fig. 2 that the main negative magnetic polarity is situated over the eastern bright region, where the higher coronal loops start; the main positive magnetic polarity is situated in part over the middle bright region, where the small loops are anchored and in part in the western boundary of NOAA 8471. We note also the presence

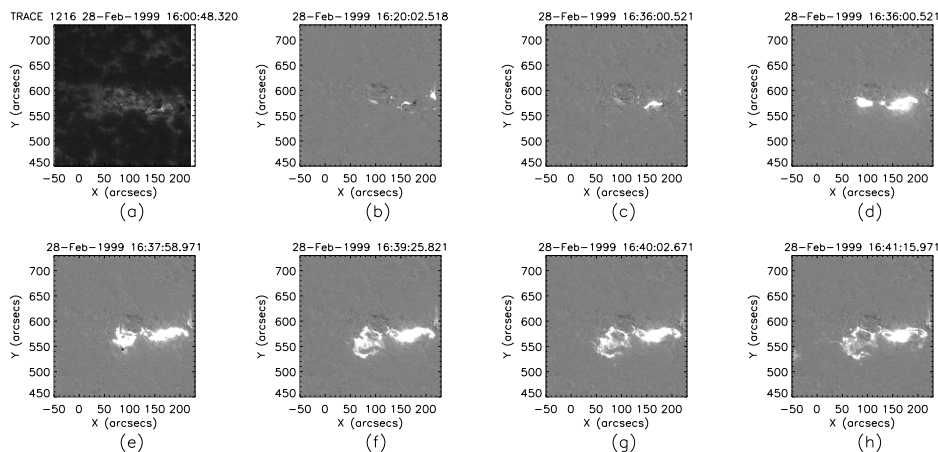


Fig. 3: 1216 Å base difference images obtained subtracting the image acquired at 16:00 UT. The range shown from white to black is ± 500 DN/s. The field of view is $2.10 \cdot 10^5 \times 2.03 \cdot 10^5$ km².

of two small negative polarity regions at $x \sim 70''$ and $y \sim 550''$ and $x \sim 100''$ and $y \sim 550''$ which were initially in close proximity to the main positive polarity, but moved rapidly eastwards following their emergence, presumably by shear flows. TRACE 171 Å loops show that these polarities appear to still be connected to the main positive polarities, but we could infer from the analysis of successive images and magnetograms that these sheared loops store considerable energy. In terms of their position, these polarities are at the interface between the western and eastern part of the highly-sheared active region, and we expect that they may play an important role in the overall flare evolution.

3. Flare evolution

A series of base difference images from the 1216 Å TRACE channel is shown in Fig. 3, where the first image, taken at 16:00 UT is the reference image used to perform the difference maps.

At 16:20 UT (Fig. 3b), at $x \sim 170''$ and $y \sim 570''$, we can see a brightness increase having a wave-like shape, which becomes more and more extended in the following images. This wave-like structure is observed at the site of filament 1. Moreover, after 1 minute and 15 seconds, (see Fig. 3c and Fig. 3d), an in-

crease of brightness appears also in the region $79'' < x < 106''$ and $567'' < y < 579''$, growing in time. We can see in Figs. 3e and 3f, that later the bright area increases along the region $60'' < x < 112''$ and $525'' < y < 590''$, where filament 2 is located. In the last two images, the brightness in the east part assumes a more dispersed shape having the appearance of an ejection or surge, while in the western part we can distinguish two ribbons.

The analysis of TRACE images acquired in the other wavelengths (1600, 171 and 195 Å) shows a similar evolution.

The analysis of BBSO H α images shows that at 16:35 UT, the filament 1 becomes brighter than the surroundings; later the area increases its brightness and extends towards the east, until it reaches the location where filament 2 is located. At 16:38 UT, the X-ray flare peak according to GOES10, the filament 2 is not visible anymore and the brightness increase is now distributed along the east-southern part of the active region, where it assumes a spray-like shape.

4. Magnetic field configuration

Fig. 4 shows the result of the potential field extrapolation obtained using the MDI magnetogram acquired at 16:03 UT. There are differ-

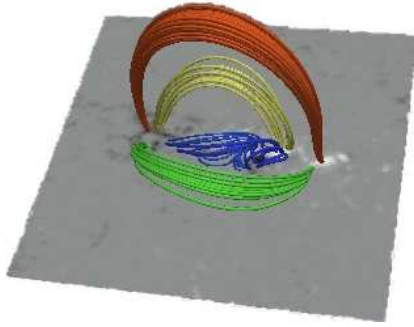


Fig. 4: Potential field extrapolation deduced using the MDI magnetogram at 16:03 UT.

ent systems of field lines, indicating the presence of higher and lower loops, that outline the loops observed at TRACE 171 Å (compare with Fig. 2).

We note four main arcades: the higher one connects the most eastern and the western polarities (red lines); another smaller arcade is situated between the most eastern negative polarity and the centered positive polarity (yellow lines); another arcade connecting the eastern negative polarity and the western positive polarity (green lines) is strongly inclined with respect to the vertical and another one much smaller, situated in the middle (blue lines), between the centered negative and positive polarities.

5. Discussion and conclusions

The results obtained from TRACE, BBSO and MDI suggest the following scenario. Filament

1, lying along a highly-sheared polarity inversion line in the main δ spot, undergoes some destabilization which results in brightening (but possibly not filament ejection). This destabilization may occur as a result of internal reconnection in the filament or interaction with surrounding field. In particular, we note that a small loop joining the central negative polarity and the main positive polarity close to the filament, rises up and appears to touch the filament just at the time of brightening. The activity in this small loop indicates that the central negative polarities are also affected by the filament activation, providing a possible link to the eastern part of the active region. In particular, one of these negative polarities is located at the end of filament 2, so reconfiguration of the linked field may result in the observed brightening and spray. The effects are dramatic because of the high shear in the core of the active region.

Acknowledgements. Financial support by the European Commission through the SOLAIRE Network (MTRN-CT-2006-035484), STFC rolling grant ST/F002637/1 and Leverhulme grant F00-179A is gratefully acknowledged.

References

- Kim, S. S., Roh, H.-S., Cho, K.-S., & Shin, J. 2006, *A&A*, 456, 747
 Rubio da Costa, F., Fletcher, L., Labrosse, N., & Zuccarello, F. 2009, *A&A*, 507, 1005